

Modification of Silicon Nanostructures by Cold Atmospheric Pressure Plasma Jets

N.S. Pokryshkin^{1,2*}, V.G. Yakunin², A.I. Efimova², A.A. Elyseev³, D.E. Presnov⁴,
V.P. Savinov², V.Yu. Timoshenko^{1,2}

¹National Research Nuclear University “MEPhI”, Phys-Bio Institute, Kashirskoe shosse, 31, Moscow, Russia

²Lomonosov Moscow State University, Faculty of Physics, Leninskie Gory, GSP-1, Moscow, Russia

³Lomonosov Moscow State University, Faculty of Chemistry, Leninskie Gory, GSP-1, Moscow, Russia

⁴D.V. Skobeltsyn Institute of Nuclear Physics, M.V. Lomonosov Moscow State University,
Leninskie gory, GSP-1, Moscow, Russia

Article info

Received:
28 January 2023

Received in revised form:
11 March 2023

Accepted:
14 April 2023

Keywords:

Nanowires
Nanostructures
Silicon
Cold atmospheric plasma
Plasma jet
Photoluminescence
Raman scattering
Charge carriers
Fano effect

Abstract

Cold atmospheric plasma (CAP) jets with helium (He) and argon (Ar) plasma-forming gases were used to modify the structure, photoluminescence (PL), and electrical properties of arrays of silicon nanowires (SiNWs) with initial cross-section sizes of the order of 100 nm and length of about 7–8 microns. The CAP source consisted of a 30 kHz voltage generator with a full power up to 5 W and the CAP treatment for 1–5 min resulted in spattering of SiNWs' tips followed by redeposition of silicon atoms. An increase of the silicon oxide phase and a decrease of the PL intensity were observed in the plasma processed SiNW arrays. A decrease of the free hole concentration and an increase in the free electron density were revealed in heavily boron and phosphorous doped SiNWs, respectively, as it was monitored by means of the Raman spectroscopy, considering a coupling of the light scattering by phonon and free charge carriers (Fano effect) in SiNWs. The obtained results demonstrate that the CAP treatment can be used to change the length, sharpness, luminescence intensity, and electrical properties of silicon nanowires for possible applications in optoelectronics and sensorics.

1. Introduction

Low-temperature gas-discharge plasma treatments are widely explored for different technological and biomedical tasks [1–6]. For example, the low-temperature plasma processing of silicon (Si) can be used for Si wafer cleaning, masked or mask-free surface texturization, and direct formation of p–n junctions for photovoltaic applications [2].

Since the gas-discharge plasma is a thermodynamically non-equilibrium medium its physical

properties are strongly dependent on the excitation and de-excitation processes, which are controlled by the electric field strength and frequency as well as gas composition and pressure [5]. Besides the low-pressure gas-discharge plasma there is a special case of as-called cold atmospheric-pressure plasma (frequently named as cold atmospheric plasma (CAP)), which is usually generated as plasma jets by compact devices [3, 4]. Commonly used CAP sources provide plasma jets enriched with various chemically reactive components [1, 4], which are promising for applications in the processing of different materials [3, 4], and in biomedicine to combat bacteria [4,6], cancer cells [7]

*Corresponding author.

E-mail address: pokryshkin.nikolay@mail.ru

and viruses [8]. It is important that the CAP treatment can be done without significant overheating of the processed object or material [1, 2].

The advantageous features of CAP for material processing are usually realized by using pulsed generators, alternating current (AC) sources of radiofrequency (13.56 MHz and its harmonics) electromagnetic radiation, and microwave power devices [9, 10]. For instance, a simple microwave CAP source consists of a generator at 2.45 GHz coupled with a tapered waveguide to increase the electric field strength required for the gas discharge ignition [11]. More sophisticated CAP devices include waveguide-to-coaxial transitions [9]. The main disadvantages of the radiofrequency and microwave systems are the high required power and size of the plasma reactor, which is often limited by waveguide dimensions, respectively [9].

AC sources, which utilize dielectric barrier discharge (DBD), are very convenient for the creation of large volume diffuse CAP [4]. While a DBD chamber can be made from a dielectric material (quartz, glass, alumina etc.), one or two electrodes are located outside the chamber that prevents their spattering in the discharge and ensures minimal contaminations of CAP [4, 9]. Such CAP sources, which are usually driven by high AC voltages at kHz frequencies, can be used for ozone generation, surface modifications, and sterilization in biomedicine [4].

Despite the impressive progress in CAP techniques and applications, a search of appropriate CAP jet sources for the controllable modification of semiconductor nanostructures is still of great importance. The present paper reports on a compact CAP jet generator operating at 30 kHz with inert discharge-forming gases, which can be used to modify the structural, optical and electrical properties of silicon nanowires (SiNWs) and it can be also used for other applications, e.g. in biomedicine.

2. Experimental

2.1. Materials

Samples of SiNWs were prepared by using a method of the metal-assisted chemical etching of crystalline Si (c-Si) wafers (see for example review [12]) with low doping levels (boron doped to the specific resistivity about $10 \Omega \text{ cm}$) and

crystallographic surface orientation of (100). The length of SiNWs was determined by the etching time and it was 7–8 μm . A part of the prepared SiNWs was subjected to additional thermo-diffusional doping with boron and phosphorous to create holes and electrons concentrations of the order of 10^{20} and 10^{19} cm^{-3} , respectively (see for details [13, 14]).

2.2. Methods

A self-made CAP source consists of a 30 kHz voltage generator powered by a DC source (voltage of 10 V), which is connected to the output stage in the form of a modernized high-voltage transformer to supply the high voltage of about 30 kV and 30 kHz frequency to the discharge gap (Fig. 1a).

The gas-discharge CAP was created between the first external electrode and a grounded metal plate (the second electrode), on which the samples were placed for plasma treatment (Fig. 1b). The plasma-forming gas (He or Ar) was supplied to the discharge gap at a rate controlled by a flow meter. The plasma jet (PJ) flowed out through a quartz tube with external and internal diameters of 5 and 3 mm, respectively, to the ambient air at atmospheric pressure. The plasma generation power was about 1 and 5 W in the case of gas-discharge in He- and Ar-flow, respectively. The CAP treatment was done for 1 and 5 min for the argon and helium plasma-forming gases, respectively.

As-prepared and plasma-processed SiNWs were analyzed by means of the scanning electron microscopy (SEM) and energy dispersive X-ray analysis (EDX) with a MAIA3 Tescan electron microscope. The structure properties of SiNWs were studied with a high-resolution Carl Zeiss Supra-40 SEM apparatus. The samples were also analyzed by means of the photoluminescence (PL) spectroscopy and Raman scattering measurements with an ATP2400 micro-spectrometer (Optosky, China) and a DFS-52 double-monochromator (LOMO, Russia), respectively. The PL signal and Raman scattering emission were excited by a UV light-emitting diode (wavelength of 365 nm, intensity of about 0.5 W/cm^2) and a He-Ne laser (wavelength of 632.8 nm, intensity of about 1 W/cm^2), respectively. The special attention was paid to avoid overheating of the samples under the laser excitation during Raman measurements.

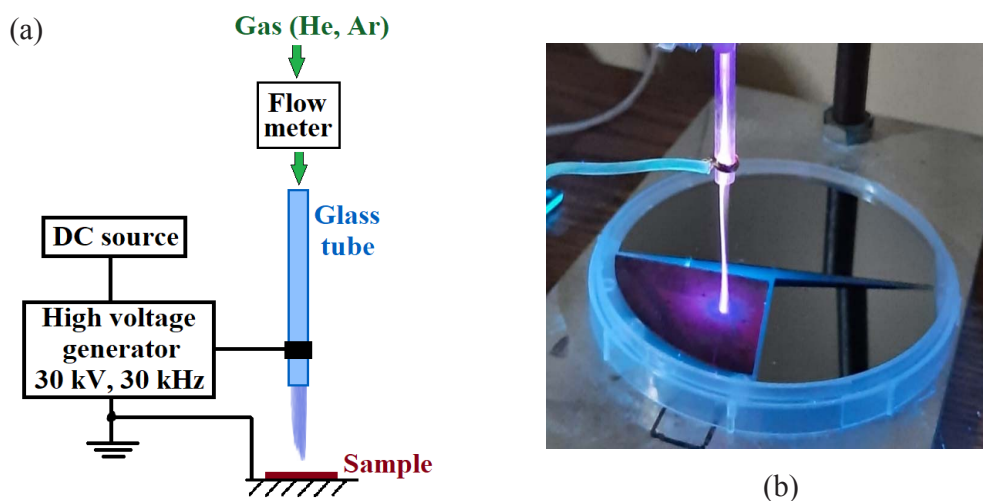


Fig. 1. (a) Schematic view of the experimental setup for the CAP generation; (b) photographic image of PJ of the used CAP source and SiNWs on c-Si wafer with under simultaneous UV excitation where the blue-red color corresponds the PL emission.

3. Results and discussion

When observing the discharge by a thermal imager, the CAP jet was not visible against the general background on its screen, while it was visible on a picture taken in day light (Fig. 1b). Thus, the employed source provided the CAP jet without hot gas flow.

Figure 2 shows typical SEM images of SiNWs before and after the CAP treatment with He and Ar plasma-forming gases. The images of side splits (Fig. 2 a, c, e) show that the structure of the nanowires is modified especially for the top layer. The top views (Fig. 2 b, d, f) show that the plasma treatment leads to a noticeable expansion of the upper parts of SiNWs.

Figure 3 shows high-resolution SEM images of the tops of SiNWs before and after He-plasma treatment, which reveal a more detailed picture of the CAP induced surface modification, i.e. expansion of SiNW's tips. The observed morphology changes were similar for the He- and Ar-plasma treatments. The modification of SiNWs was a kind of volume expansion of the upper parts leading to the mushroom-like shape of the nanowires. The structure change of SiNWs can be explained by an effect of high local electric fields at SiNW' tips under the CAP treatment that causes a sputtering of Si atoms. Indeed, even a small voltage drop (1–10 V) on a nanoscale can create the a field strength of the order of 10^5 – 10^6 V/cm. As an example of the destructive effect of the electric field of CAP, one

can cite the well-known results of the destruction of a living cell when a voltage of 1 V applied to the cell membrane is enough to cause pore formation in the latter [15, 16].

The chemical content of SiNWs was estimated by using the EDX analysis. Typical EDX spectrum of SiNWs after the CAP treatment with Ar-forming gas is shown in Fig. 4. Similar changes in the PL spectra were also obtained for the CAP treatments with He-forming gas.

The EDX analysis showed that the PJ-treatment resulted in a significant increase in the oxygen content in the treated samples. The amount of oxygen on the surface of the sample increases from 18 at.% to 40 at.%. The observed significant surface oxidation of SiNWs is explained by an interaction of the PJ-sputtered Si-atoms with molecular oxygen in ambient air. So, the observed volume expansion of SiNWs and mushroom-shaped porous morphology formation can be caused not only by amorphization, but also by the oxidation of silicon.

Figure 5 shows PL spectra of SiNWs under UV excitation recorded before and after CAP treatment. The red PL of SiNWs is usually associated with radiative transitions in small Si nanocrystals on SiNWs' surfaces (see for example [17]). The PL quenching can be explained by both quenching of the luminescent centers on the SiNWs' surfaces and the appearance of new nonradiative defects due to fast solidification and oxidation of Si nanoclusters. The increase of oxidized fraction was confirmed by the EDX measurements (see Fig. 4).

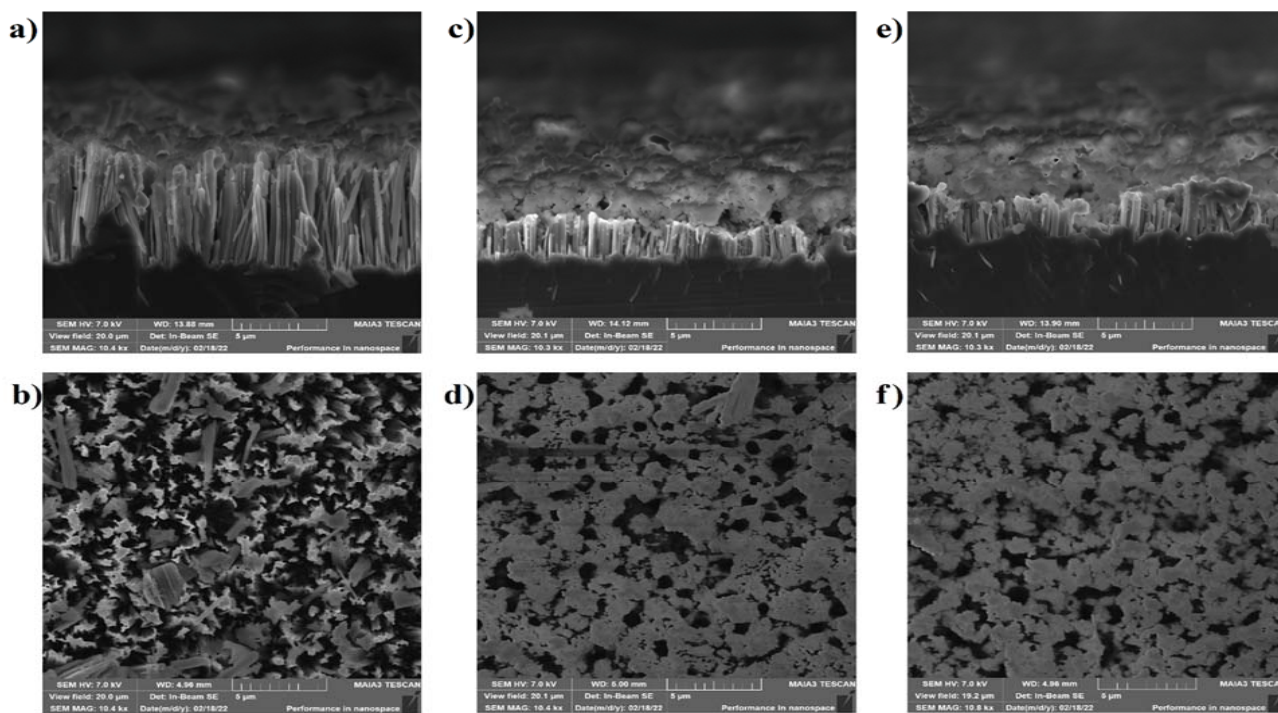


Fig. 2. SEM cross-sectional images (a, c, e) and top-views (b, d, f) of SiNWs before (a, b) and after CAP treatment with He (c, d) and Ar (e, f).

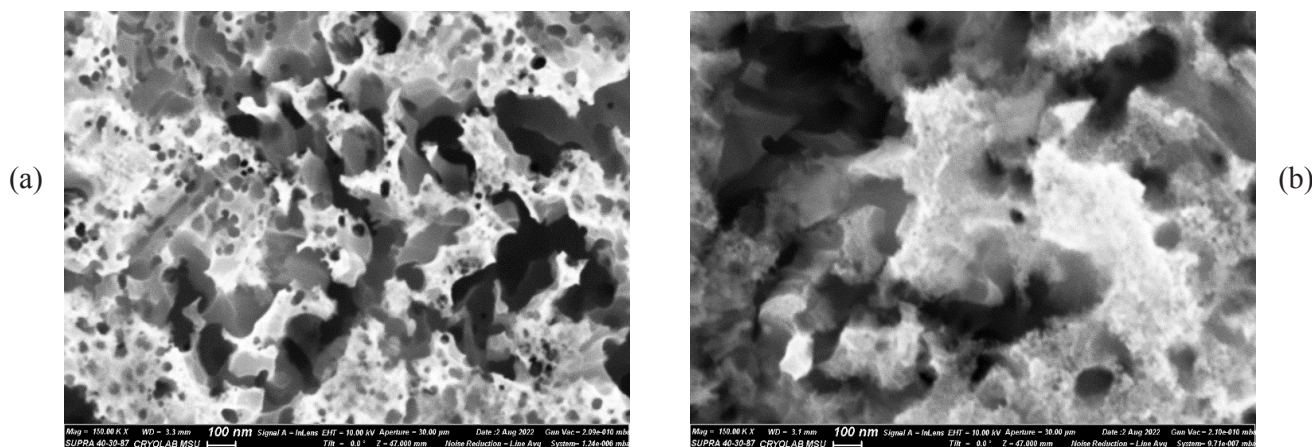


Fig. 3. High-resolution SEM top-view images of SiNWs' tips before (a) and after (b) CAP-treatment.

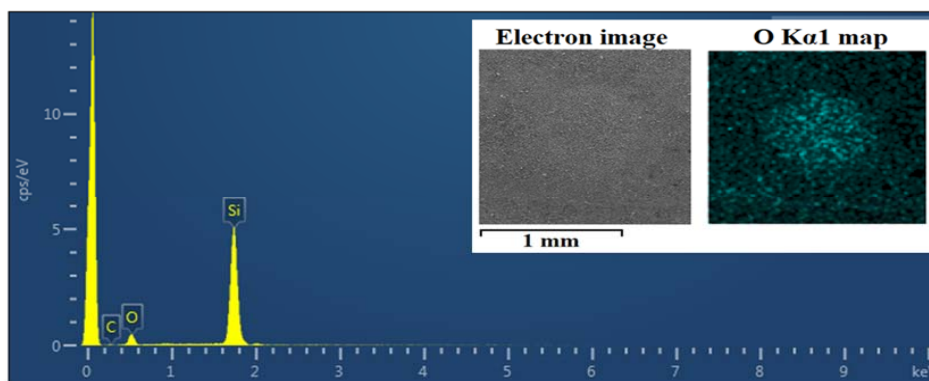


Fig. 4. Typical EDX spectrum of a CAP-treated region of SiNWs. Left and right insets show a SEM image and EDX map of the CAP-treated region of the sample.

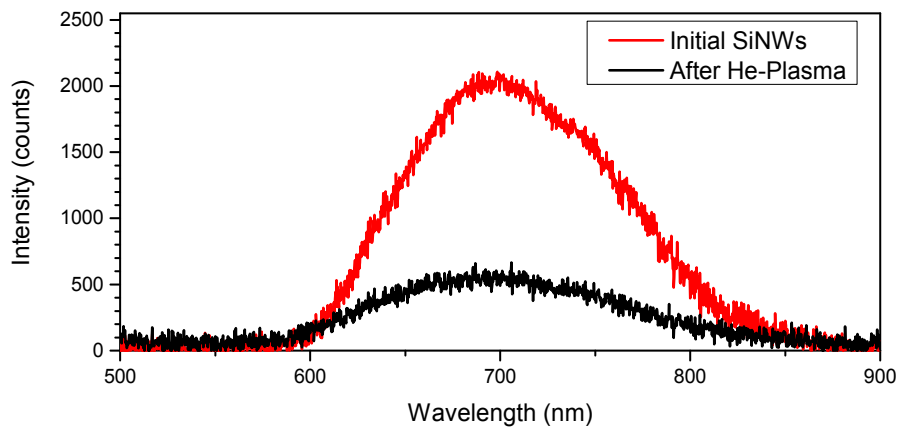


Fig. 5. PL spectra of SiNWs before and after CAP treatment with He plasma-forming gas for 5 min.

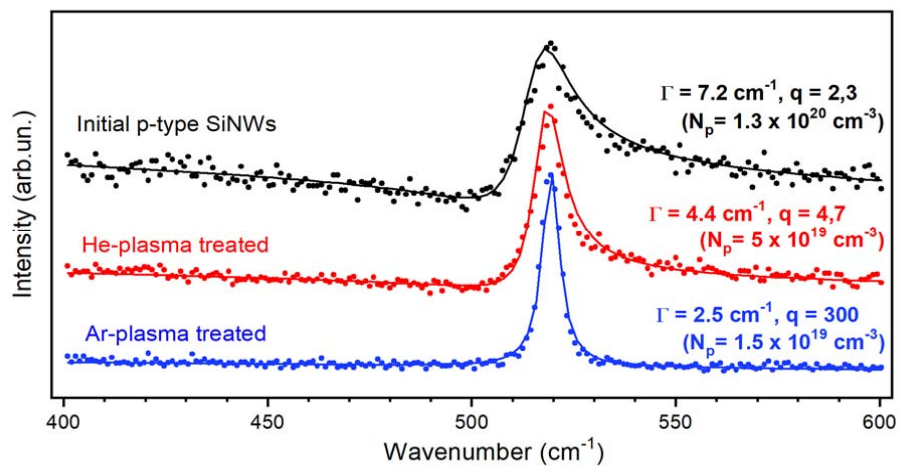


Fig. 6. Raman spectra of the initial sample and CAP-treated p-type SiNWs. Experimental data are plotted by points, while solid lines are fits by using Eq. 1 with parameters and free hole concentrations indicated near the corresponding curves.

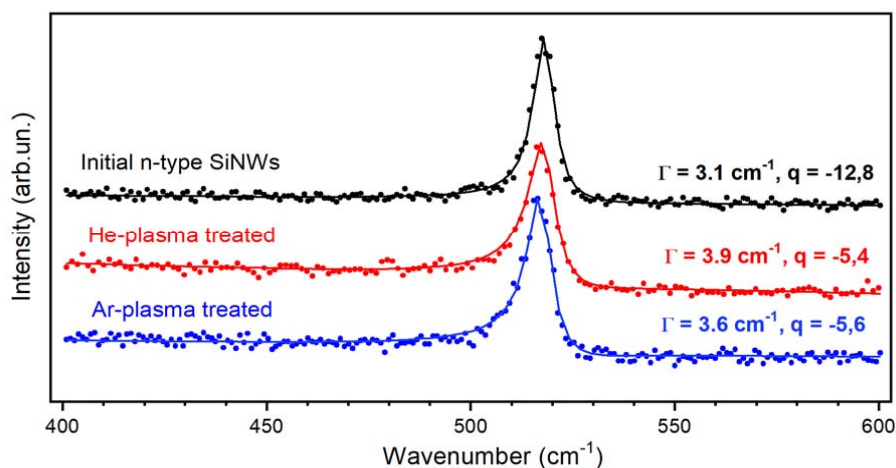


Fig. 7. Raman spectra of the initial sample and CAP-treated n-type SiNWs. Experimental data are plotted by points, while solid lines are fits by using Eq. 1 with parameters indicated near the corresponding curves.

Additional information about the plasma processing of Si-nanostructures can be obtained by using the Raman spectroscopy data for p-type and

n-type doped SiNWs as shown in Figs. 6 and 7, respectively.

The initial Raman spectrum of p-type SiNWs is broadened and modified due to the Fano effect [18], which is related to a coupling between the phonons and free charge carriers (holes) as it is well known for heavily doped p-type c-Si [19].

It is known that a one-phonon Raman spectrum in the heavily doped p-type c-Si [20] and SiNWs [21] can be described by the following Fano-like shape:

$$I(\varepsilon, q) = C \frac{(q + \varepsilon)^2}{1 + \varepsilon^2}, \quad (1)$$

where $\varepsilon = (\omega - \omega_0)/\Gamma$, ω is the wavenumber, q is the asymmetry parameter, Γ is the line width, ω_0 is the phonon wavenumber and C is an intensity coefficient.

Free charge carriers (holes in case of p-type doping) influence the line width in the following way [21]:

$$\Gamma = C_1 + C_2 N_p^{\frac{1}{3}}, \quad (2)$$

where C_1 , C_2 are empirical coefficients, N_p is the concentration of positive free charge carriers (holes).

The asymmetry parameter of the Raman spectra is also dependent on the concentration of free holes according to the following expression [21]:

$$q^{-1} = C_3 + C_4 N_p^{\frac{1}{2}}, \quad (3)$$

where C_3 , C_4 are empirical coefficients.

CAP treatments with He- and Ar plasma-supporting gases for 1–5 min were found to reduce the asymmetry and broadening of the Raman spectra of p-type SiNWs. These spectral changes are especially pronounced in the case of Ar-treatment (blue curve in Fig. 6). Since the width and asymmetry of the phonon Raman line are related to charge carrier density, the CAP treatment results in a decrease of the concentration of positive charge carriers (holes) in p-type SiNW by one order of magnitude as shown in Fig. 6. It was found that SiNWs after prolonged CAP treatment (more than 5 min) exhibited further decrease of the free hole concentration up to an undetectable level below 10^{18} cm^{-3} . This fact can be explained by the growing concentration of the compensating defects in the CAP treated samples.

The effect of CAP treatment on n-type SiNWs, on the contrary, enhances the width and asymmetry of the observed Raman peak (Fig. 7). Note, the plasma-treated samples exhibit both the smaller absolute values and low-wavenumber shift of their Raman spectra (red and blue curves in Fig. 7). This fact can be explained by an increase in the concentration of negatively charged free carriers (electrons) that is well known for the Fano effect in the Raman scattering in n-type c-Si [22]. Because of small changes in the line shape it is difficult to estimate exact values of the free electron concentration in n-type SiNWs. However, the strongly asymmetric shape of the Raman spectrum of the CAP treated n-type SiNW sample indicates the free electron concentration above $5 \cdot 10^{19} \text{ cm}^{-3}$ [22]. The plasma-induced n-type doping of c-Si was observed in several studies (see for examples review [2] and Ref. [23]) and it was proposed to form p-n-junction in Si-wafer with initial p-type conductivity [2].

As for the origin of the plasma-induced n-type conductivity in c-Si it can be explained by oxygen-related defects (as-called thermal donors) in oxygen-rich c-Si regions [2]. The thermal donor formation can be also responsible for the observed strong increase in the free electron concentration in SiNWs according to the observed Fano-shape of their Raman scattering line (see Fig. 7). In fact, the additional oxidation of SiNWs was detected after the CAP treatment (see Fig. 4).

The observed CAP modification of SiNWs can be compared with the results of pulsed laser treatments of porous Si films when clear evidences of the laser-induced melting of Si nanostructures were found [24, 25]. Indeed, the pulsed laser irradiation even with nanosecond pulses resulted in the strong heating and melting of Si nanostructures, which are characterized by low thermal conductivity [24]. In this respect, the cold plasma treatment can be used as a unique fine tool for the non-thermal modifications of Si nanostructures.

4. Conclusions

Finally, a self-made cold atmospheric plasma source with inert plasma-forming gas was constructed and used for the modification of the morphology, photoluminescence, and electrical properties of silicon nanowire arrays on c-Si substrate. The cold plasma treatment of SiNWs was found to

result in the sputtering of their tips followed with Si-atoms redeposition and oxidation in surrounding air. As a result of the cold plasma treatment, the red photoluminescence of SiNWs was suppressed and it was probably related to the disappearance of the luminescent Si nanocrystals and the generation of new nonradiative defects on the SiNWs' surfaces. The Raman spectroscopy revealed the significant changes in the line shape of the one-phonon Raman line in the samples of plasma processed heavily doped SiNWs, which indicated a strong decrease of the free hole density and increasing the free electron concentration for p-type and n-type samples, respectively. The obtained results indicate that the compact and relatively simple CAP source can be used to modify the structure, luminescence and electrical properties of Si-based nanowires in a controllable way due to the plasma sputtering of surface atoms. The obtained results can be used for the development of cold-plasma methods for the treatment of Si-nanostructures for optoelectronic and sensor applications, e.g. local surface oxidation, p-n-junction formation etc.

Acknowledgments

The authors acknowledge E.A. Lipkova and A.S. Eremina for their assistance in the preparation of doped samples of silicon nanowires and SEM measurements, respectively. In the course of this work, the research infrastructure of the «Educational and Methodical Center of Lithography and Microscopy», M.V. Lomonosov Moscow State University was used.

References

- [1]. M.G. Kong, M. Keidar, K. Ostrikov. *J. Phys. D: Appl. Phys.* 44 (2011) 174018. DOI: [10.1088/0022-3727/44/17/174018](https://doi.org/10.1088/0022-3727/44/17/174018)
- [2]. S.Q. Xiao, S. Xu, K. Ostrikov. *Mater. Sci. Eng. R Rep.* 78 (2014) 1–29. DOI: [10.1016/j.mser.2014.01.002](https://doi.org/10.1016/j.mser.2014.01.002)
- [3]. Ch. Ma, A. Nikiforov, D. Hegemann, et al., *Int. Mater. Rev.* 68 (2022) 82–119. DOI: [10.1080/09506608.2022.2047420](https://doi.org/10.1080/09506608.2022.2047420)
- [4]. M. Laroussi, *Front. Phys.* 8 (2020) 1–7. DOI: [10.3389/fphy.2020.00074](https://doi.org/10.3389/fphy.2020.00074)
- [5]. K. Ostrikov, E.C. Neyts, M. Meyyappan, *Adv. Phys.* 62 (2013) 113–224. DOI: [10.1080/00018732.2013.808047](https://doi.org/10.1080/00018732.2013.808047)
- [6]. G.A. Gruzdev, O.V. Karpukhina, V.G. Yakunin, et al., *Moscow Univ. Biol. Sci. Bull.* 76 (2022) 244–248. DOI: [10.3103/S0096392521040027](https://doi.org/10.3103/S0096392521040027)
- [7]. C. Almeida-Ferreira, R. Silva-Teixeira, M. Laranjo, et al., *Appl. Sci.* 11 (2021) 4171. DOI: [10.3390/app11094171](https://doi.org/10.3390/app11094171)
- [8]. Zh. Chen, G. Garcia, V. Arumugaswami, R.E. Wirz, *Phys. Fluids* 32 (2020) 111702. DOI: [10.1063/5.0031332](https://doi.org/10.1063/5.0031332)
- [9]. L. Bárdos, H. Baránková, *Thin Solid Films* 518 (2010) 6705–6713. DOI: [10.1016/j.tsf.2010.07.044](https://doi.org/10.1016/j.tsf.2010.07.044)
- [10]. F. Bu, S. Feyzi, G. Nayak, et al., *Innov. Food Sci. Emerg. Technol.* 83 (2023) 03248. DOI: [10.1016/j.ifset.2022.103248](https://doi.org/10.1016/j.ifset.2022.103248)
- [11]. K.M. Green, M.C. Borrás, P.P. Woskov, et al., *IEEE Trans. Plasma Sci.* 29 (2001) 399–406. DOI: [10.1109/27.922753](https://doi.org/10.1109/27.922753)
- [12]. H. Han, Z. Huang, W. Lee, *Nano Today* 9 (2014) 271–304. DOI: [10.1016/j.nantod.2014.04.013](https://doi.org/10.1016/j.nantod.2014.04.013)
- [13]. S.P. Rodichkina, T. Nychyporuk, A.V. Pavlikov, et al., *Phys. Status Solidi A* 2017 (2020) 1900670. DOI: [10.1002/pssa.201900670](https://doi.org/10.1002/pssa.201900670)
- [14]. S.P. Rodichkina, T. Nychyporuk, A.V. Pavlikov, et al., *J. Raman Spectrosc.* 50 (2019) 1642. DOI: [10.1002/jrs.5702](https://doi.org/10.1002/jrs.5702)
- [15]. K.H. Schoenbach, F.E. Peterkin, R.W. Alden, S.J. Beebe, *IEEE Trans. Plasma Sci.* 25 (1997) 284–292. DOI: [10.1109/27.602501](https://doi.org/10.1109/27.602501)
- [16]. E. Sysolyatina, A. Mukhachev, M. Yurova, et al., *Plasma Process. Polym.* 11.4 (2014) 315–334. DOI: [10.1002/ppap.201300041](https://doi.org/10.1002/ppap.201300041)
- [17]. V.Yu. Timoshenko, K.A. Gonchar, L.A. Golovan, et al., *J. Nanoelectron. Optoelectron.* 6 (2011) 519–524. DOI: [10.1166/jno.2011.1205](https://doi.org/10.1166/jno.2011.1205)
- [18]. U. Fano, *Phys. Rev.* 124.6 (1961) 1866. DOI: [10.1103/PhysRev.124.1866](https://doi.org/10.1103/PhysRev.124.1866)
- [19]. F. Cerdeira, T.A. Fjeldly, M. Cardona, *Phys. Rev. B* 8 (1973) 4734–4745. DOI: [10.1103/PhysRevB.8.4734](https://doi.org/10.1103/PhysRevB.8.4734)
- [20]. B.G. Burke, J. Chan, K.A. Williams, et al., *J. Raman Spectrosc.* 41.12 (2010) 1759–1764. DOI: [10.1002/jrs.2614](https://doi.org/10.1002/jrs.2614)
- [21]. A.I. Efimova, E.A. Lipkova, K.A. Gonchar, et al., *J. Raman Spectrosc.* 51 (2020) 2146–2152. DOI: [10.1002/jrs.5956](https://doi.org/10.1002/jrs.5956)
- [22]. M. Chandrasekhar, J.B. Renucci, M. Cardona, *Phys. Rev. B* 17 (1978) 1623–1633. DOI: [10.1103/PhysRevB.17.1623](https://doi.org/10.1103/PhysRevB.17.1623)
- [23]. A.N. Buzynin, A.E. Luk'yanov, V.V. Osiko, V.V. Voronkov, *Nucl. Instrum. Methods Phys. Res. B* 186 (2002) 366–370. DOI: [10.1016/S0168-583X\(01\)00882-5](https://doi.org/10.1016/S0168-583X(01)00882-5)
- [24]. V.Y. Timoshenko, T. Dittrich, I. Sieber, et al., *Phys. Status Solidi A* 182 (2000) 325–330. DOI: [10.1002/1521-396X\(200011\)182:1<325::AID-PSSA325>3.0.CO;2-%23](https://doi.org/10.1002/1521-396X(200011)182:1<325::AID-PSSA325>3.0.CO;2-%23)
- [25]. T.R. Northen, H.-K. Woo, M.T. Northen, et al., *J. Am. Soc. Mass. Spectrom.* 18 (2007) 1945–1949. DOI: [10.1016/j.jasms.2007.08.009](https://doi.org/10.1016/j.jasms.2007.08.009)